Published in final edited form as:
Proc SPIE Int Soc Opt Eng. 2005 February ; 5747(3): 2110–2117. doi:10.1117/12.595450.

Artifact reduction in truncated CT using Sinogram completion

R. Chityala[@,d,e], **K. R. Hoffmann**[a,c,d], **S. Rudin**[a,b,c,d,e], and **D. R. Bednarek**[a,b,c,d,e]

[a]Department of Physics, State University of New York at Buffalo, 3435 Main Street, Buffalo, NY 14214

[b]Department of Radiology, State University of New York at Buffalo, 3435 Main Street, Buffalo, NY 14214

[c]Department of Neurosurgery, State University of New York at Buffalo, 3435 Main Street, Buffalo, NY 14214

[d]Toshiba Stroke Research Center, Rm 445, Biomedical Research Building, State University of New York at Buffalo, 3435 Main Street, Buffalo, NY 14214

[e]Erie County Medical Center, 462 Grider Street, Buffalo, NY 14215

Abstract

Truncation of projection data in CT produces significant artifacts in the reconstruction process due to non-locality of the Radon transform. In this paper, we present a method for reducing these truncation artifacts by estimating features that lie outside the region of interest (ROI) and using these features to complete the truncated sinogram.

Projection images of an object are obtained. A sinogram is obtained by stacking profile data from all projection angles. A simulated truncated sinogram is generated by setting pixel values outside an ROI to zero. The truncated sinogram is then transformed into a (radius, phase) image, with pixel values in what we term as the Polar representation (PR) image corresponding to the minimum value along sine curves given by x = r*cos(projection angle + phase). The PR image contains data for radii greater than the ROI radius. Pixel values outside the ROI in the completed sinogram are determined as follows. For each pixel in the PR image, a sine curve is generated in the completed sinogram image outside the ROI, having the same pixel value as that of the PR image for that radius and phase. Successive sine curves are laid and the values of each are summed. The intensity outside is then equalized to the intensity inside the ROI. The completed sinogram is then reconstructed, to obtain completed reconstruction.

The percentage error in the difference image between the full FOV reconstruction and the corresponding completed reconstruction and the extrapolated-average reconstruction are 1.1% and 3.3% respectively. This indicates that the completed reconstruction is closer to full FOV reconstruction. Thus, the sinogram completion can be used to improve reconstructions from truncated data.

[@]Corresponding author: chitvala@buffalo.edu; Tel: 716-829-3595 xll4; Fax: 716-829-2212..

Keywords

Sinogram completion; truncated reconstruction; Sinogram; extrapolation; artifact reduction; dose reduction; reduced FOV

1. INTRODUCTION

If the field of view for a Computed Tomography (CT) scan were collimated to include only a region of anatomic interest, the integral dose to the patient could be reduced. However CT reconstruction suffers from truncation artifacts if the scan field of view (FOV) is smaller than the size of the object to be imaged due to non-locality of the Radon transform. The truncation artifacts are characterized by bright bands at the edge of the FOV, obscuring the anatomy around the edge. It also results in a severe "inverse cupping" artifact, reducing contrast at points inside the FOV. Various approaches have been proposed to reduce these artifacts by estimating or determining data outside the FOV, and hence reduce the truncation artifact. These may be classified into four categories.

The first category of methods to overcome truncation artifact estimates the data outside the ROI. Hsieh[1] presented an approach for extending the FOV by using the property that the total attenuation of each projection in a parallel-beam geometry remains constant over the views. Ohnesorge et al[2], developed an extrapolation procedure, in which the data outside the ROI was smoothed, so that the intensity dropped at a slower rate. The hybrid detruncation[3] (HDT) algorithm backprojects the data and completes the missing portions of the truncated sinogram using the reconstructed data. An algebraic technique[4] involving multiple backprojection and projection operations has been proposed to overcome these truncation artifacts. Wiegert[5] proposed a reconstruction technique in which the truncated data acquired during intervention was combined with the previously acquired 3D data of the same anatomy covering the whole object. An optical means of determining the data outside the FOV was proposed by Wagner[6].

The second category aims at identifying and eliminating objects[7] that corrupt the data inside the ROI (The term ROI is used synonymously with FOV) in the projection images and removes them to obtain better reconstruction inside the ROI.

A third category of ROI techniques called "Local Tomography" was developed by Faridani, et al.[8,9], which reconstructs using the data along lines very close to the point of interest. However the reconstructed image from local tomography does not represent the map of the attenuation coefficients, but only the edges and boundaries.

A fourth category[10,11] of algorithm acquires data outside the ROI but at a reduced dose.

In this paper, we propose an extrapolation technique which takes advantage of the fact that every feature in the object traces a sine curve in the sinogram. By completing the sine curves in a truncated sinogram, we can obtain reconstruction comparable to full FOV inside the ROI. The truncated sinogram is decomposed into individual sine curves by mapping the projection space into (r, φ) space using a process similar to backprojection. The truncated sinogram is completed using the (r, φ) space image and then reconstructed. The technique was tested on two categories of data sets. In the first set of data, the image had stent alone, which was a clearly identifiable high contrasts object. The second data set was the image of a head phantom, which did not have any identifiable high contrast objects in the ROI.

2. ROI IMAGE ACQUISITION

The projection images for the study were acquired using the system shown in Figure 1.

The system specifications used for obtaining the stent images were

1. An Oxford Ultra-Bright x-ray tube (Oxford Instruments PLC, Scotts Valley, CA, USA) with a focal spot of 40 microns using 90 kV, 2 mA and an exposure time of 300 ms.
2. A detector[10] that utilizes a 2D CCD camera and has a field of view (FOV) of approximately 5 cm × 5 cm. The pixel size is 43 microns with an image size of 1024 × 1024 and bit depth of 12.
3. A Tri-Star stent (Guidant Corporation, Indianapolis, IN, USA).

The system specifications used for obtaining the images of head phantom were

1. Infinix C- Arm system (Toshiba Medical Systems Corporation, Tokyo, Japan).
2. An image-intensifier-based detector with a pixel size of 270 microns and an image size of 1024 × 1024.
3. A human head phantom (The Phantom Laboratory, Salem, NY).

For both data sets, a rotary stage with degree precision better than 0.1 was used to acquire images every 2° for a full 360° rotation; thus, 180 projection images were acquired. As indicated in Figure 1, the x-ray source and detector are stationary, and the object is rotated.

3. METHODS

3.1 Sinogram decomposition

Let the Radon transform of a given function $f(x,y)$ be denoted as $R[f]$,

$$R\left[f\left(x,y\right)\right]=\int\int f\left(x,y\right)\delta\left(x\cos\theta+y\sin\theta-x'\right)dxdy=P\left(x',\theta\right) \quad (1)$$

where $P(x', \theta)$ is the projection image as indicated in Figure 2.

Reconstruction can be performed by finding the inverse Radon transform which can be written mathematically as

$$f\left(x,y\right)=R^{-1}\left[P\left(x',\theta\right)\right] \quad (2)$$

When the entire object is imaged in all projections, the inverse Radon transform yields the original object (to within the limitations of resolution and noise statistics). When truncated projections (i.e., projections with incomplete data outside an ROI) are obtained, objects at radii larger than that of the ROI appear in some projections and not in others. Thus, the truncated projection data are inconsistent, and result in artifacts due to non-locality of the Radon transform.

To overcome the truncation artifacts, we propose to estimate the data outside the ROI using the information within the ROI. The method makes use of the sinogram, which is a two-dimensional data set consisting of the projection data $P(x',\theta)$ for all x' and θ. For this study, a truncated sinogram, resulting from an ROI smaller than the object, is obtained by assigning a value of zero outside the ROI in the projection image. To estimate the data in the region outside the ROI, we transform the truncated sinogram data from (x', θ) space to (r, φ) space, where r is the radius from the center of rotation (isocenter) and φ is the phase angle (the angle made by the vector joining the feature and the isocenter with the x-axis), as shown in Figure 3. The transformation relating the two spaces is given by

$$x^{'}=r\cos\left(\theta+\phi\right) \quad (3)$$

For non-truncated sinograms, the transformation for back projection would normally involve summation along each sine curve, after the application of a ramp filter to each projection. This summation is placed at the (r, φ) location to obtain the reconstructed image. This (r, φ)image is the polar representation of the reconstructed image.

However, for the truncated sinogram, this approach leads to artifacts due to inconsistent data. In an attempt to overcome these artifacts, we use a non-linear approach in which we determine the minimum attenuation value along the sine curve and use that value for the (r, φ) location in the image. We designate this image as the “polar representation image”, $PR(r,\varphi)$.

For a discrete case, the decomposition process can be defined mathematically as

$$PR\left(r,\phi\right)=\min_{x^{'},\theta}\left(S\left(x^{'},\theta\right)^{*}I\left(x^{'},\theta\right)\right) \quad (4)$$

where $S(x', \theta)$ is the truncated sinogram, and $I(x', \theta)$ is a function defined as

$$I\left(x^{'},\theta\right)=\begin{cases}1 & \forall \quad x^{'}=r\cos\left(\theta+\phi\right)\\ 0 & otherwise\end{cases} \quad (5)$$

The intensity of a point in the PR image is determined by the minimum value on the sine curve. This assumes that, if the feature corresponding to the sine curve does not overlay any other feature, will directly give the attenuation coefficient corresponding to that feature. Thus, every point in the PR image corresponds to a sine curve in the projection image and its intensity will be the minimum attenuation value along that sine curve.

3.2 Selection of sinogram completion parameters

When fitting a sine curve, error in estimation of the phase of the sine curve results in translation of the sine curve whereas error in estimation of radius of the sine curve results in distortion of the sine curve. Hence the PR image is blurred in the radial direction but not in the phase direction. Thus at a very high radius in comparison to the ROI radius, the blurring will be high. This limits the size of the radius of completion in relation to the ROI radius. For the case of stent wires, which had fewer and well defined high contrast objects, 4 times the size of the ROI radius was chosen. For the head phantom, which did not have well defined features, 2 times the size of the ROI radius was chosen.

To determine the range of intensity values of the sine that will be completed, we generate the histogram of the PR image. The pixels in the top 10% intensities of the histogram (corresponding to the high contrast objects) are completed in the sinogram.

3.3 Sinogram completion method

To evaluate the method,

1. A truncated sinogram (Figure 4b) is created from a full FOV sinogram (Figure 4a) by setting the data outside the ROI to zero; it is then log converted to obtain a sinogram in attenuation space.
2. The underlying constant background is removed by subtracting, the minimum attenuation value inside ROI from all points inside the ROI, to obtain a subtracted sinogram. This is done so that high contrast structures inside the ROI are highlighted.
3. For each point (r, φ) in the PR image (Figure 5), and for each projection angle (θ), the corresponding coordinate in the subtracted sinogram is generated using Equation 3.
4. The minimum intensity value along each of these sine curve inside the ROI is determined in the truncated sinogram and is assigned to the point (r, φ) in the PR image.
5. Steps 3 and 4 are repeated until all points in the PR image are used.
6. The sinogram is then completed outside the ROI by using the PR image. For every point (r, φ) in the PR image, a sine curve is generated outside the ROI which corresponds to that point in the truncated sinogram. The sine curves are chosen based on two parameters: the radius at which the sine curve is located in the PR image and its intensity value. The selection of these two parameters are described in Section 3.2.
7. The individual sine curves are continued and added in the region outside the ROI. Hence the intensity outside the ROI may be greater than that inside, if there is a superposition of sine curves at some locations in the sinogram. Thus, the intensities must be equalized prior to back-projection. This is done by assuming a linear relationship in the intensities inside and outside the ROI, in the vicinity of the ROI boundary. We average the intensity values close to the edge of the ROI both inside

(I_{in}) (3 pixels inside the edge) and outside (I_{out}) (3 pixels outside the edge) for all the projection angles. We then obtain the mapping function by fitting I_{out} (x-axis) and I_{in} (y-axis) and the region outside the ROI is equalized to obtain the equalized sinogram.

8. The minimum value (corresponding to the background) subtracted in Step 2 is then added back to the equalized sinogram (Figure 6) and the image is then reconstructed from the resultant sinogram. This reconstructed image will be referred as the "*completed reconstruction*."

For comparison, an *extrapolated-average reconstruction* was performed by assigning the average intensity of each projection angle inside the ROI to all points for the same projection angle in the region outside ROI in the sinogram. It was observed by Van Gompel et al[7] that completing the data outside the ROI using a smooth function can improve reconstruction substantially inside the ROI. The extrapolated-average reconstruction was performed as a first approximation to smoothing the data outside the ROI.

3.3 Metrics

Qualitative metrics such as details visible and artifact reduction in the reconstructed ROI were used to compare the effectiveness of sinogram completion. For quantitative comparison, the difference image between the full FOV reconstructions and the truncated and extrapolated-average reconstruction were obtained. The mean square error (MSE) value between the full FOV reconstruction and other two reconstructions was calculated inside the ROI. Percentage error (PE) defined as the ratio of MSE to the intensity of the structure (stent or bone) in the reconstructed image was also calculated.

4. RESULTS & DISCUSSION

4.1 Results for stent only case

The minimum value inside the ROI for a sinogram of the projections of a stent alone is zero, so that the subtracted sinogram is the same as the truncated sinogram. In Figure 7a–7e, we present the results for reconstruction using the sinogram of the stent image. The high-contrast point-like objects in the full FOV reconstruction (Figure 7a) correspond to the individual stent wires. The circle at the center corresponds to the selected ROI region. The stent wire inside the ROI for the reduced FOV is reconstructed using both methods: Figure 7b is the sinogram completed reconstruction and Figure 7c is the extrapolated-average reconstruction. Figure 7d and 7e are the corresponding difference images. The MSE (Table 1) in Figure 7d is 32.2, and the PE (calculated with reference to the intensity of stent wires in the reconstructed image) is 0.37%, while the corresponding values for the extrapolated-average reconstruction (Figure 7e) are 68.1 and 0.76%, indicating that reliable reconstruction can be obtained from sinogram completed reconstruction. It also indicates that the reconstruction using sinogram completion is superior to the extrapolated-average reconstruction. The difference image in Figure 7d and 7e look similar qualitatively but differ quantitatively due to the cupping artifact.

4.2 Results for head phantom

The head phantom has a non-zero minimum (i.e. background) inside the ROI. Hence before decomposition, a subtracted sinogram (Figure 8) is created.

Figure 9 is the PR image of the head phantom. The PR image is obtained by decomposing (determining the minimum value along the sine curve) the subtracted sinogram (Figure 8) of the head phantom after subtracting the minimum intensity at all points inside the ROI, so that high contrast features are highlighted.

The completed sinogram is created after equalizing the intensity between inside and outside and also after adding the minimum value subtracted from the truncated sinogram.

In Figures 11, we present the results for reconstruction of the head phantom. The circle at center of the full FOV reconstruction (Figure lla) indicates the region inside the ROI. The completed reconstruction and extrapolated-average reconstruction are shown in Figure 11b & 11e respectively, with the corresponding difference image in Figure 11d & 11e. The MSE (Table 1) for completed reconstruction is 25.0, and the PE (calculated with reference to the intensity of bone in the reconstructed image) is 1.1%, while the corresponding values for the extrapolated-average reconstruction (Figure 11e) are 75.2 and 3.3%. Both the techniques appear to provide fairly accurate reconstructions, even though the region outside the ROI was estimated. The improvement provided by the completed-reconstruction indicates that this technique provides more information than the extrapolated-average reconstruction. The difference image in Figure 11d and 11e look similar qualitatively but differ quantitatively due to the cupping artifact.

5. CONCLUSION

Reduced FOV provides a way to reduce the integral dose to the patient, when acquiring the images of an ROI. However, truncated reconstruction results in severe artifacts at the edge of the ROI. These artifacts can be reduced using sinogram completion by extrapolating the “ROI” data in the region outside the ROI. We found that the technique performs for both high as well as low contrast objects and provides reconstruction within 1% of the full FOV reconstruction. It also improves the reconstruction in comparison to a simple estimate of the data outside the ROI.

The method described here is still under active investigation for improvements. These results are promising, with further improvements in the quality of reconstruction expected upon investigation of the effects of the methods to generate the PR image, the equalization technique, and the completion technique.

ACKNOWLEDGMENTS

This work was supported by NIH Grant numbers: R01NS38746, R01HL52567, R01EB002916, R01NS43924, and R01EB002873. The authors would like to acknowledge Guidant Corporation for providing the stents and the Toshiba Medical Systems Corporation for an equipment grant.

REFERENCES

1. Hsieh J, Chao E, Thibault J, Grekowicz B, Horst A, McOlash S, Myers TJ. A novel reconstruction algorithm to extend the CT scan field-of-view. Med Phys. Sep; 2004 31(9):2385–91. [PubMed: 15487717]
2. Ohnesorge B, Flohr T, Schwarz K, Heiken JP, Bae KT. Efficient correction for CT image artifacts caused by objects extending outside the scan field of view. Med Phys. Jan; 2000 27(1):39–46. [PubMed: 10659736]
3. Penssel, C.; Kachelriess, M.; Kalender, WA.; Sourbelle, K. Hybrid Detruncation (HDT) Algorithm for the Reconstruction of CT Data. RSNA; Chicago: 2004. p. 293
4. Zhao S, Jaffray D. Iterative Reconstruction-Reprojection for Truncated Projections. Med Phys. Jun. 2004 31(6):1719.
5. Wiegert J, Bertram M, Wulff J, Schaefer D, Weese J, Netsch T, Schomberg H, Rose G. 3D-R0I Imaging for Cone-Beam Computed Tomography. Proceedings of CARS. 2004; 1268:7–12.
6. Wagner W. Reconstructions from restricted region scan data – New means to reduce the patient dose. IEEE Transactions on Nuclear Science. Apr.1979 NS-26(2)
7. Van Gompel G, Tisson G, Van Dyck D, Sijbers J. A new algorithm for Region Of Interest Tomography. SPIE Medical Imaging : Image Processing. 5370:2105–2113.
8. Faridani A, Ritman EL, Smith KT. Local Tomography. SIAM. J. Appl. Math. Apr; 1992 52(2):459–484.
9. Faridani A, Ritman EL, Smith KT. Examples of Local Tomography. SIAM. J. Appl. Math. Aug; 1992 52(4):1193–1198.
10. Chityala R, Hoffmann KR, Bednarek DR, Rudin S. Region of interest (ROI) computed tomography (CT): Comparison with full field of view (FFOV) and truncated CT for a human head phantom. SPIE. 2005
11. Rudin, S.; Wu, Y.; Kyprianou, I.; Ionita, C.; Wang, Z.; Ganguly, A.; Bednarek, DR. Proceedings of SPIE 2002: Physics of Medical Imaging. Vol. 4682. SPIE; San Diego, CA: Micro-angiographic detector with fluoroscopic capability; p. 344-353.

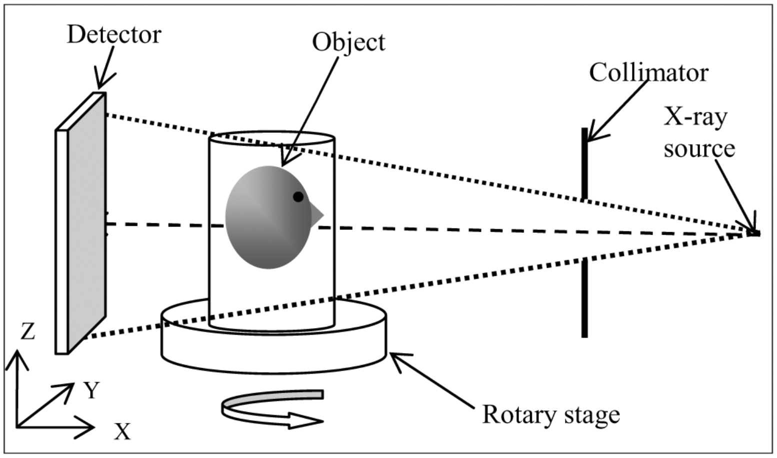

Figure 1.
Schematic of the setup for image acquisition

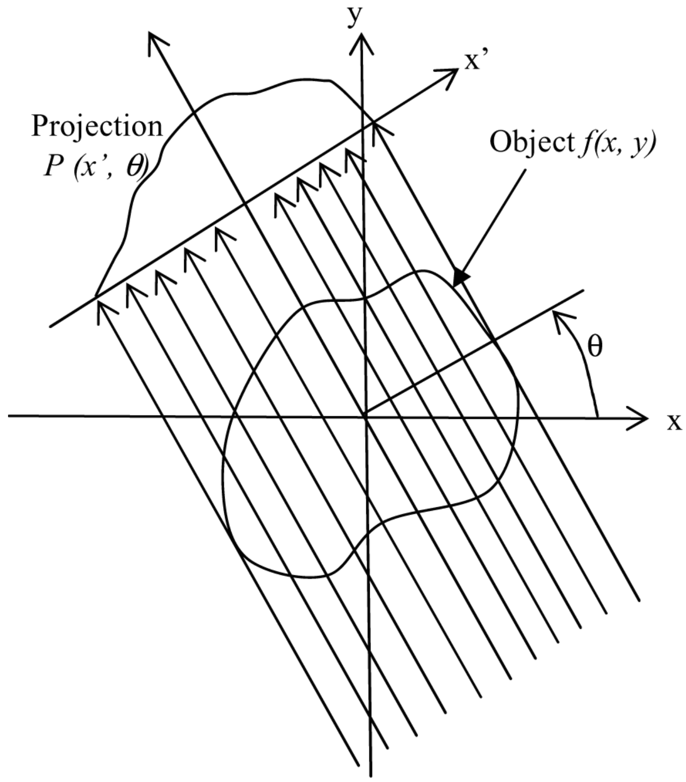

Figure 2.
Pictorial representation of the image acquisition corresponding to a distribution f(x, y)

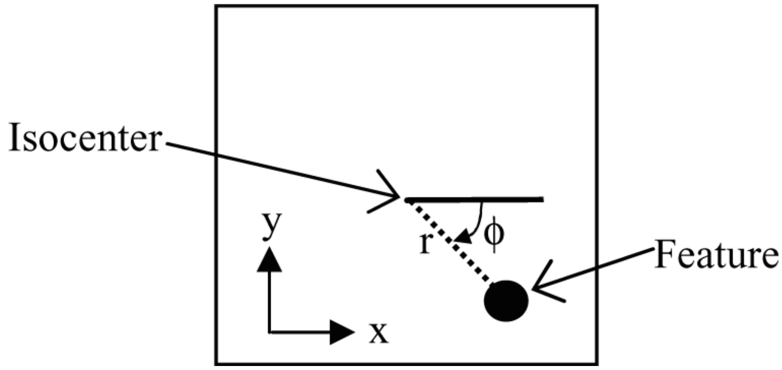

Figure 3.
Schematic diagram showing the definition of r and φ on a reconstructed image.

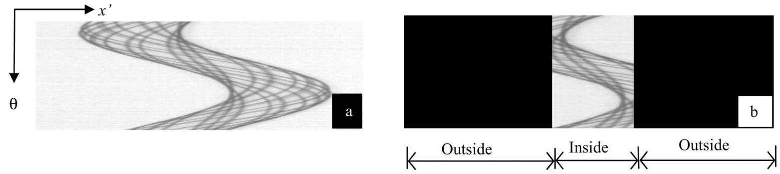

Figure 4.
The left image (Figure 4a) is the Full FOV sinogram of a stent consisting of a number of wires. The right image (Figure 4b) is the truncated sinogram. Note that the region outside the ROI is zero corresponding to a truncated sinogram in which there is no data acquired outside the ROI.

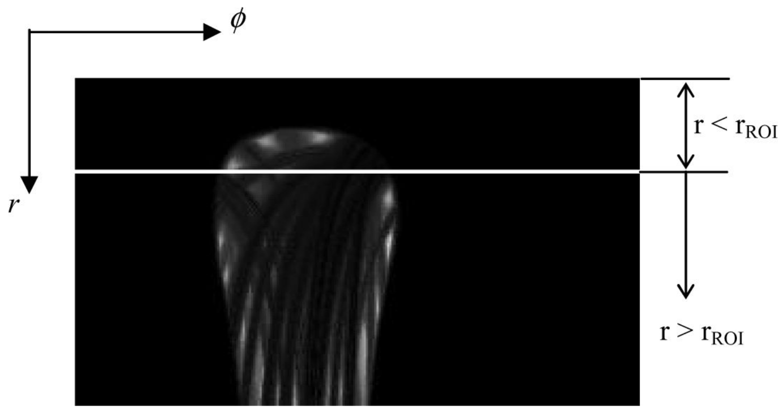

Figure 5.

The PR image having the minimum intensity along each sine curve The points with high intensity correspond to the sine curves of the stent wires. The rROi is the radius of ROI.

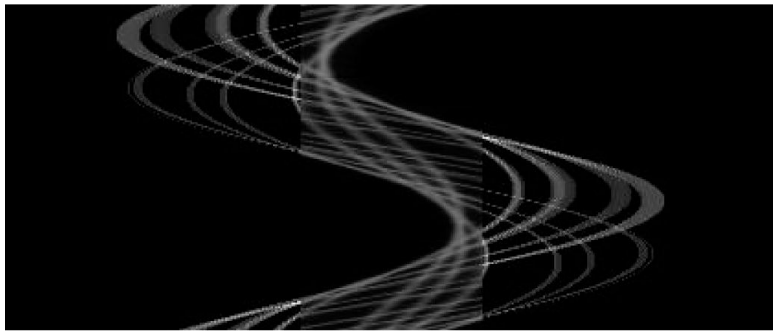

Figure 6.
The completed sinogram. To evaluate the quality of completion, compare this sinogram with the full FOV sinogram (Figure 4a).

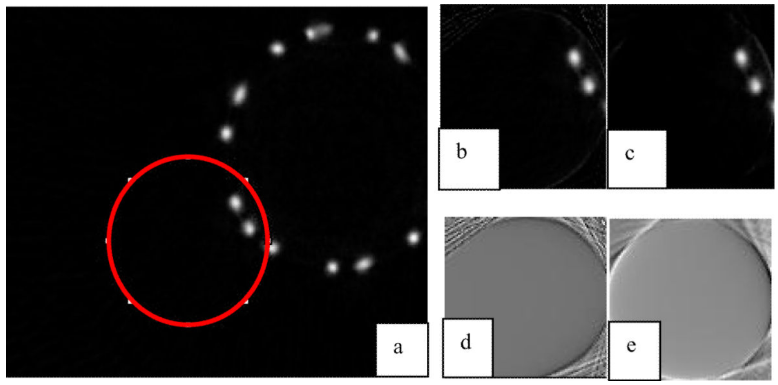

Figure 7.

Reconstructed image of stent wires. (a) The reconstruction obtained using the full FOV data. (b) The reconstruction obtained using sinogram completion. (c) The reconstruction obtained using extrapolated-average estimation. (d) The difference image between the full FOV and completed reconstructions. (e) The difference image between the full FOV and extrapolated average reconstructions. The display contrast in d and e is 100 times that of a, b, and c.

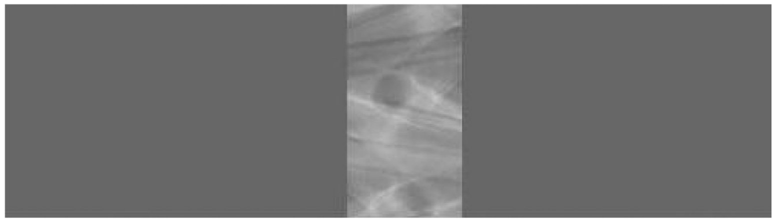

Figure 8.
Subtracted sinogram of the head phantom.

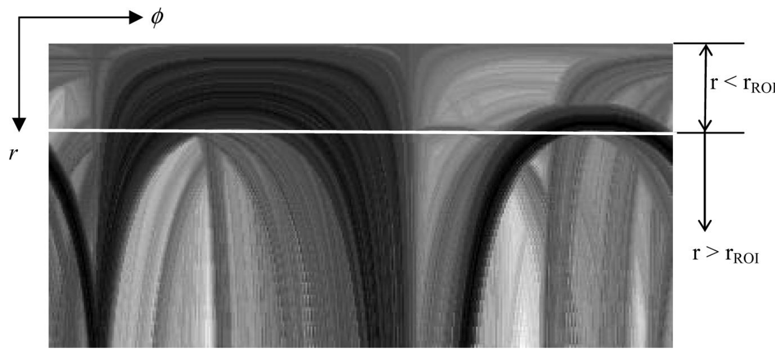

Figure 9.

The PR image of the subtracted sinogram. Points in the PR image with high intensity correspond to the high contrast features in the subtracted sinogram. The rROi in the figure is the radius of ROI.

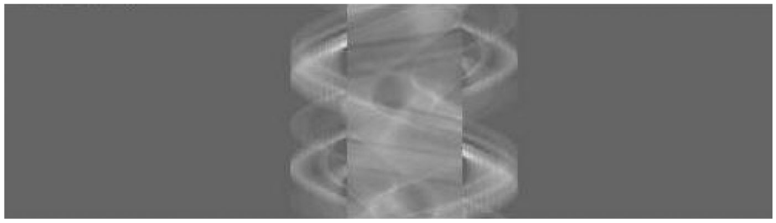

Figure 10.
Completed sinogram.

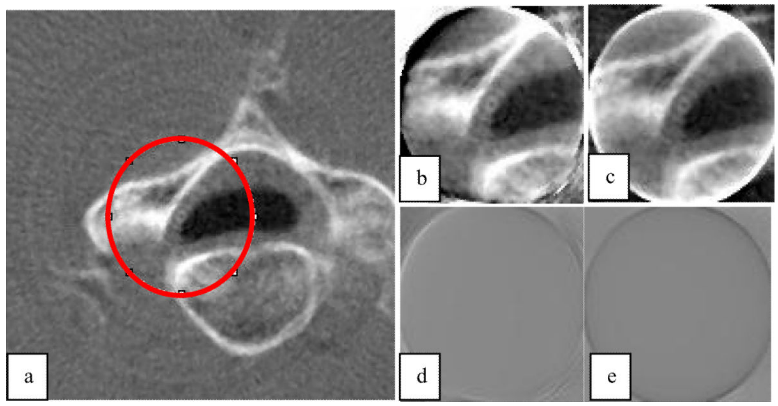

Figure 11.

Reconstructed image of head phantom. (a) The full FOV reconstruction. (b) The sinogram-completed reconstruction. (c) The extrapolated-average reconstruction. (d) The difference image between the full FOV reconstruction and the completed reconstruction. (e) The difference image between the full FOV reconstruction and the extrapolated-average reconstruction. The contrast in d and e is 100 times that of b and c. The ring artifact at the center of the image is a result of detector gain differences which can be corrected using a flat field acquisition.

Table 1

The MSE and PE for the difference image between the two reconstructions and the full FOV reconstruction

	Completed reconstruction		Extrapolated-average reconstruction	
	Sent only	**Head phantom**	**Stent only**	**Head phantom**
MSE	32.2	25.0	68.1	75.2
PE (%)	0.37	1.1	0.76	3.3